Intracranial hemorrhage segmentation using a 3D U-Net with squeeze-and-excitation blocks

Valeriia Abramova, Albert Clèrigues, Liliana Valencia, Uma Lal-Trehan, Marc Guirao, Arnau Oliver, Joaquim Salvi, and Xavier Lladó

Computer Vision and Robotics Group, University of Girona, Catalonia, Spain

Abstract. Intracranial hemorrhage is a dangerous condition characterized with high mortality rates. Early and accurate diagnosis is a key factor in its successful treatment. Non-contrast Computed Tomography is the most common imaging modality used in hemorrhagic stroke diagnosis. In this work, a deep learning-based approach to automatically segment hemorrhagic stroke lesions in CT scans is proposed. Our approach is based on a 3D U-Net architecture which incorporates squeeze-and-excitation blocks. Moreover, we also analyzed the effect of patch size and the use of symmetric modality augmentation on the segmentation results. All analyses have been performed using a five fold cross-validation strategy on a dataset of 100 cases provided within the INSTANCE 2022 International challenge. The results obtained on the validation set of 30 cases show a Dice score of 0.693 ± 0.284, showing promising automated segmentation results.

Keywords: Hemorrhagic stroke · Computed Tomography · Segmentation · Deep Learning.

1 Introduction

Intracranial hemorrhage (ICH) is a type of stroke which involves a rupture of a vessel inside the brain and it is characterized with a high mortality rate [1]. Early diagnosis is crucial in hemorrhage treatment and positive patient's outcome. Computed tomography (CT) is usually used for stroke diagnosis as it can satisfy this condition being rapid but widely available medical imaging tool. Although it allows pretty accurate diagnosis of ICH, the correct estimation of lesion volume is challenging yet very important for hematoma growth and outcome prediction [2]. In clinical practice, ABC/2 is the commonly used method for hematoma volume calculation [3], however, it has its own limitations, like volume estimation error because of irregular lesion shape, different locations, low contrast, difference in scanners, etc. Hence, it is important to provide an automated tool for ICH segmentation, which will allow accurate volume quantification.

Nowadays, Convolutional Neural Networks (CNNs) showed good results for hematoma segmentation [4, 5]. However, precise ICH segmentation still remains a challenging task because of its variations in shapes and locations. In this paper we propose a CNN approach for automatic ICH segmentation that will be evaluated

with the MICCAI INSTANCE2022 challenge [6, 7]. Our approach is based on our previous work, where we used a 3D-Unet with the incorporation of squeeze-and-excitation blocks [8].

2 Materials and methods

2.1 Dataset

The MICCAI INSTANCE2022 challenge dataset consists of 100 non-contrast CT images provided as a training set and 30 cases for open validation dataset. 70 remaining cases will be used as a closed testing dataset [6, 7]. All the examinations were performed on an TOSHIBA Aquilion ONE CT scanner and the size of each CT volume is 512×512×N, where N is between 20 and 70 [7]. The pixel spacing of each CT volume is 0.42mm×0.42mm×5mm. The images in the training and validation datasets will be used for evaluation and for deciding the best algorithm configuration for the testing phase of the challenge. The gold reference standard consisted of the masks of the hemorrhagic stroke lesions manually delineated by 10 expert radiologists on the non-contrast CTs. Each case was labeled by 5 radiologists and results were then merged together using a voting strategy. Examples of cases showing the variety of hemorrhages present in the dataset are shown in Figure 1.

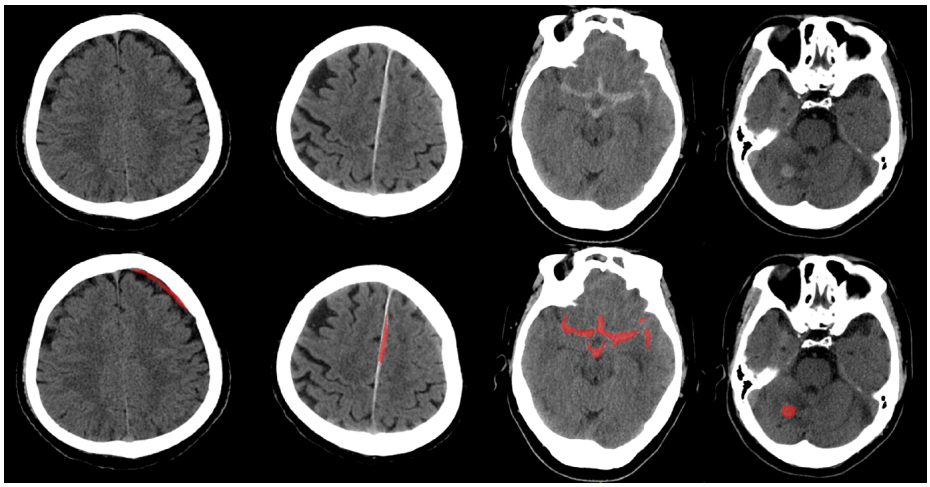

Fig. 1. Examples of cases of the proposed dataset. Intracranial hemorrhages in the challenge dataset are of different shapes, locations, size, and contrast with the brain tissue. The original images are shown in the top row and with the groundtruth overlaid in the bottom row.

2.2 Data preparation

The preprocessing of the non-contrast CT images requires coil removal and skull stripping as these regions might confound the network behavior and lead to inappropriate results. The coil removal was done using morphological operations, and skull stripping was done similarly to [9], where the brain region was extracted using morphological operations to remove the border of the skull and subsequently extracting the largest connected component. The resulting brain volume was processed slice by slice to find the slice containing the largest brain tissue area, which we define as $Slice_{max}$. Thus, the brain regions in the slices above $Slice_{max}$ were determined as largest connected components of brain tissue. For the slices below the $Slice_{max}$, the brain region extracted from the preceding slice was used as a mask to extract the brain region from the subsequent slice.

For the normalization of input images, we performed percentile based range adjustment. Similarly to [10], we used 0.5 and 99.5 percentiles of brain-related voxels for clipping together with image-based calculated mean and standard deviation normalization.

Since typically some subtypes of stroke occur within one brain hemisphere, it could be useful to utilize features based on the mid-sagittal symmetry of the brain, as proposed in [11], to evaluate the difference between brain hemispheres and to better detect the hematoma. Therefore, to study the effect of utilizing this property, a symmetric image was created for each case by flipping the original non-contrast CT and registering it to the initial one using the FLIRT algorithm from the FSL toolbox [12, 13].

2.3 Patch sampling

For ICH segmentation task, class imbalance can be an issue. Hence, in our approach we used a balanced sampling patch extraction technique, where we extracted an equal number of patches representing both classes from each image. To avoid extracting a lot of patches from image background, we restricted the area to extract the negative patches within the brain mask. Therefore, the patch extraction pipeline is set up as following. Firstly, we set a target number of patches to extract from each image in the training set. Half of them are uniformly extracted from the brain tissue area and represent negative class, while the other half is extracted from the lesion voxels.

2.4 U-net with squeeze-and-excitation blocks

Similarly to our previous work [8], we utilize a 3D U-Net with incorporation of squeeze-and-excitation blocks, as such architecture showed improved performance for the hemorrhage segmentation task. We use single 3×3×3 convolutions in both contracting and expansive paths and rectified linear unit (ReLU) as activation function. Down-sampling in each level is performed by a 2×2×2 max pooling operation with a stride of 2, followed by dropout. In the decoding path, the upsampling is performed with up-convolution of 2×2×2 with a stride of 2,

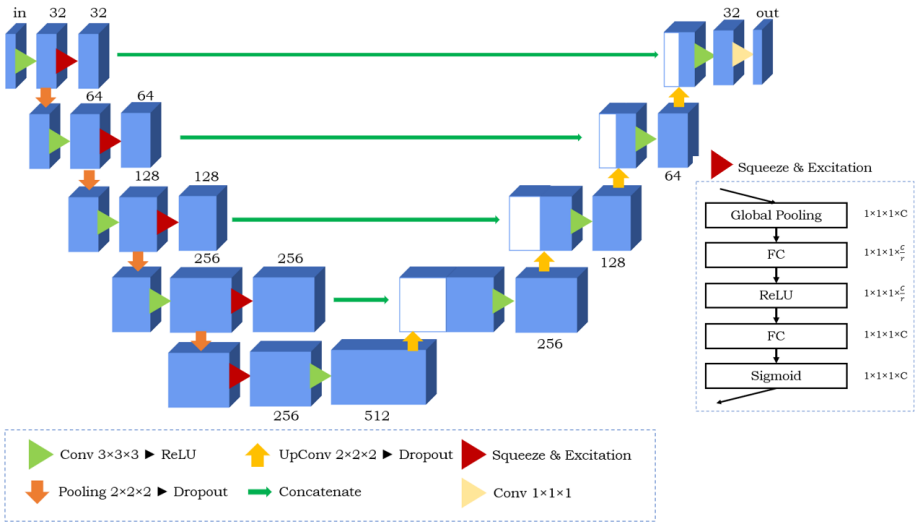

Fig. 2. The 3D architecture used in the proposed approach. The network is inspired by a 3D U-Net with incorporation of squeeze-and-excitation blocks. Blue blocks represent feature maps with a number of channels stated above or below them. Red triangles represent the location, where we incorporate squeeze-and-excitation operations. In the detailed description of these operations, C and r represent the number of input channels and reduction ratio, respectively.

followed by dropout. We propose to incorporate squeeze-and-excitation blocks after each level in the encoding path, as shown in a Figure 2. The details on our experimental setup are provided in the following section.

2.5 Training and validation pipelines

In the training stage, we augment the proposed dataset by choosing difficult cases and adding them into the training set again, meanwhile performing flipping and rotation, ensuring that more difficult patches are generated for training. Afterwards, we divided proposed scans into training and validation set with a proportion of 80% of scans for training and 20% for validation. From each image, 3000 patches of the size $48 \times 48 \times 16$ were extracted following the balanced sampling patch extraction technique introduced previously. As a loss function, the combination of Dice and Cross-entropy losses was used together with Adadelta optimizer, as these parameters showed improved performance with a similar task of ICH segmentation [8]. In the cross-entropy loss, the weight for lesion class was doubled to give more weight to difficult examples in the dataset. To prevent overfitting, we used early stopping technique with patience tolerance of 10 when approaching the minimal loss on validation set. All the experiments were performed with a 5-fold cross-validation across all cases of the provided training dataset.

For the validation and testing stages, an ensemble with all the 5 models obtained in the cross-validation experiment was used to generate the final prediction masks. The probability masks obtained from the 5 models were averaged and thresholded to obtain the final binary mask for each case.

2.6 Postprocessing

Considering the results on the validation set, postprocessing was added to our pipeline to reduce the number of false positives. As sizes of lesions vastly vary in the provided images, we perform postprocessing taking into account the volumes of the lesions in the segmentations we obtained. That is, for each image we find the biggest lesion and calculate its volume. Afterwards, in the postprocessed image, we remove all the lesions with the volume less than 10% of the biggest one.

3 Experimental results

To optimize the performance of the proposed pipeline, we performed different experiments. For instance, the effect of incorporation of squeeze-and-excitation (SE) blocks into different parts of the network was studied. We performed experiments with SE blocks after encoding and decoding paths, as in [8], with SE blocks after ever encoder and decoder blocks and with SE blocks after each level in the encoding path. The experimental results showed that the best results were obtained when squeeze-and-excitation blocks were incorporated after each level in the encoding path, increasing the mean DSC by 3.5%. Such configuration of the neural network was used in the rest of experiments.

We also studied the influence of different patch sizes on the segmentation results. Three patch sizes were tested - (16, 16, 8), (32, 32, 8) and (48, 48, 16). Considering the results obtained when using the provided training set and when using the validation set at the validation stage, we finally chose the patch size of (48, 48, 16) to be used in the final submission. Even though training with this patch size did not introduce much improvement for small lesions, it could notably improve the segmentation of other cases.

Moreover, we analyzed the influence of adding the symmetric version of the original image on the segmentation results. Even though in most cases hematoma presents in one hemisphere of the brain, some of the images show other hematoma subtypes, which can affect both hemispheres. As a result, providing symmetric image as an additional input channel did not show any significant improvement of the obtained segmentation results.

We also test the influence of different image normalization techniques. The image range was adjusted using the minimum and maximum values of the image and, in another experiment, based on percentiles. From the experiments done, percentile based range adjustment for input images provided better results than range adjustment based on minimum and maximum, being combined with other

modifications. Only changing the input normalization technique ensured a 1% increase in Dice score in the training set.

Finally, we also studied if making our proposed U-Net deeper could improve the obtained results. Our experiments, showed that making U-Net one level deeper can improve segmentation results, increasing the resulting Dice score to 0.712 ± 0.257 in the training set and reaching 0.693 ± 0.284 at the validation stage, being our best result.

Taking into account all the previous experiments, the final configuration of the proposed method was chosen. The network architecture was a 4-levels U-Net which included squeeze-and-excitation blocks after each level in the encoding path. The network was trained with 3000 patches of size $(48, 48, 16)$ using as a loss function the combination of Dice and cross-entropy losses. Percentile-based image normalization was applied to input images without performing symmetric modality augmentation. With this final design, we achieved the Dice score of 0.693 ± 0.284 in the validation stage of INSTANCE 2022 challenge.

4 Conclusion

In this work we proposed a deep learning method for hemorrhagic stroke lesions segmentation in CT images that was evaluated with the data of the INSTANCE 2022 challenge. The proposed approach, based on a patch based 3D U-Net architecture with integration of squeeze-and-excitation blocks, was tested on the provided training dataset with 100 cases. The obtained results were qualitatively and quantitatively evaluated on the whole dataset using a 5-fold cross-validation strategy obtaining a Dice of 0.712 ± 0.257. Our final approach was also evaluated on the 30 images of the validation set, reaching a Dice of 0.693 ± 0.284, and will be tested on the 70 images of the testing dataset.

5 Acknowledgments

Valeriia Abramova and Albert Clèrigues hold FPI grants from the Ministerio de Ciencia, Innovación y Universidades with reference numbers PRE2021-099121 and PRE2018-083507, respectively. This work has been supported by DPI2020-114769RB-I00 from the Ministerio de Ciencia, Innovación y Universidades and also by the ICREA Academia program. The authors gratefully acknowledge the support of the NVIDIA Corporation with their donation of the TITAN X GPU used in this research.

References

1. Heit, J.J., Iv, M., Wintermark, M.: Imaging of Intracranial Hemorrhage. J Stroke. 19, 11–27 (2017). https://doi.org/10.5853/jos.2016.00563
2. de Oliveira Manoel, A.L., Goffi, A., Zampieri, F.G., Turkel-Parrella, D., Duggal, A., Marotta, T.R., Macdonald, R.L., Abrahamson, S.: The critical care management of spontaneous intracranial hemorrhage: a contemporary review. Crit Care. 20, 272 (2016). https://doi.org/10.1186/s13054-016-1432-0

3. Chinda, B., Medvedev, G., Siu, W., Ester, M., Arab, A., Gu, T., Moreno, S., D'Arcy, R.C.N., Song, X.: Automation of CT-based haemorrhagic stroke assessment for improved clinical outcomes: study protocol and design. BMJ Open. 8, e020260 (2018). https://doi.org/10.1136/bmjopen-2017-020260
4. Hssayeni, M.D., Croock, M.S., Salman, A.D., Al-khafaji, H.F., Yahya, Z.A., Ghoraani, B.: Intracranial Hemorrhage Segmentation Using a Deep Convolutional Model. Data. 5, 14 (2020). https://doi.org/10.3390/data5010014
5. Hu, K., Chen, K., He, X., Zhang, Y., Chen, Z., Li, X., Gao, X.: Automatic segmentation of intracerebral hemorrhage in CT images using encoder–decoder convolutional neural network. Information Processing & Management. 57, 102352 (2020). https://doi.org/10.1016/j.ipm.2020.102352
6. X. Li, G. Luo, W. Wang, K. Wang, Y. Gao and S. Li: Hematoma Expansion Context Guided Intracranial Hemorrhage Segmentation and Uncertainty Estimation. IEEE Journal of Biomedical and Health Informatics **26**(3) 1140–1151 (2022) https://doi.org/10.1109/JBHI.2021.3103850
7. Li, X., Wang, K., Liu, J., Wang, H., Xu, M., Liang, X.: The 2022 Intracranial Hemorrhage Segmentation Challenge on Non-Contrast head CT (NCCT). (2022) https://doi.org/10.5281/zenodo.6362221
8. Abramova, V., Clèrigues, A., Quiles, A., Figueredo, D.G., Silva, Y., Pedraza, S., Oliver, A., Lladó, X.: Hemorrhagic stroke lesion segmentation using a 3D U-Net with squeeze-and-excitation blocks. Computerized Medical Imaging and Graphics. 90, 101908 (2021). https://doi.org/10.1016/j.compmedimag.2021.101908
9. Vidya, M.S., Mallya, Y., Shastry, A., Vijayananda, J.: Recurrent Sub-volume Analysis of Head CT Scans for the Detection of Intracranial Hemorrhage. In: Shen, D., Liu, T., Peters, T.M., Staib, L.H., Essert, C., Zhou, S., Yap, P.-T., and Khan, A. (eds.) Medical Image Computing and Computer Assisted Intervention – MICCAI 2019. pp. 864–872. Springer International Publishing, Cham (2019). https://doi.org/10.1007/978-3-030-32248-9_96
10. Isensee, F., Jaeger, P.F., Kohl, S.A.A., Petersen, J., Maier-Hein, K.H.: nnU-Net: a self-configuring method for deep learning-based biomedical image segmentation. Nat Methods. 18, 203–211 (2021). https://doi.org/10.1038/s41592-020-01008-z
11. Clèrigues, A., Valverde, S., Bernal, J., Freixenet, J., Oliver, A., Lladó, X.: Acute ischemic stroke lesion core segmentation in CT perfusion images using fully convolutional neural networks. Computers in Biology and Medicine. 115, 103487 (2019). https://doi.org/10.1016/j.compbiomed.2019.103487
12. Jenkinson, M., Bannister, P., Brady, M., Smith, S.: Improved optimization for the robust and accurate linear registration and motion correction of brain images. Neuroimage. 17, 825–841 (2002). https://doi.org/10.1016/s1053-8119(02)91132-8
13. Jenkinson, M., Smith, S.: A global optimisation method for robust affine registration of brain images. Med Image Anal. 5, 143–156 (2001). https://doi.org/10.1016/s1361-8415(01)00036-6